Journal of Alloys and Compounds 275–277 (1998) 669–676

Rare earth phosphors: fundamentals and applications

C.R. Ronda*, T. Jüstel, H. Nikol

Philips GmbH Forschungslaboratorien Aachen, P.O. Box 500145, D-52085 Aachen, Germany

Abstract

In this paper an overview is given of luminescent materials, based on rare earth ions. Fundamental aspects and classical applications of luminescent materials applied in fluorescent lamps and displays are discussed with regard to optical properties. The application potential of rare earth phosphors with regard to new developments such as phosphors for LEDs and luminescent materials with quantum yield larger than unity is also discussed. © 1998 Elsevier Science S.A.

Keywords: Rare earth phosphors; Quantum cutter

1. Introduction

Luminescent materials, also called phosphors, are mostly solid inorganic materials consisting of a host lattice, usually intentionally doped with impurities. The absorption of energy takes place via either the host lattice or on impurities. In addition, transfer of energy through the lattice can take place. In almost all cases, the emission originates from impurities.

Luminescent materials are widely applied today. Major applications are in emissive displays and fluorescent lamps. In addition, some X-ray detector systems are based on luminescent materials as well.

In the last decades, a large number of luminescent materials based on rare earth ions or rare earth host lattices has been invented. Quite a few of these materials also found their way into applications. In many cases, rare earth phosphors dramatically improved the performance of the devices in which they are applied.

In the first part of this paper, the emission properties of rare earth ions are discussed and compared to the emission properties of other luminescent ions or molecular groups. The second part deals with applications of luminescent materials with emphasis on rare earth phosphors. The paper ends with a discussion of new developments in the field of rare earth phosphors in the third part.

2. Emission properties of rare earth ions in comparison to other emitting centers

In most cases, the emission of rare earth ions is due to optical transitions within the f-manifold (e.g. Tb^{3+} ($4f^8$), Gd^{3+} ($4f^7$) and Eu^{3+} ($4f^7$). The f-electrons are well shielded from the chemical environment and therefore have almost retained their atomic character. As a consequence, the f–f emission spectra consist of sharp lines. In addition, the f–f transitions are partially forbidden and many of them are also spin forbidden. Therefore, these optical transitions are generally very slow, viz. in the range of microseconds to milliseconds.

For a number of rare earth ions, however, also broad emission bands are known. Prominent examples are Eu^{2+} ($4f^7$) and Ce^{3+} ($4f^1$). In this case, emission is due to 5d–4f optical transitions. As d electrons participate in the chemical bonding, the d–f emission spectra consist of broad bands. Furthermore, the d–f optical transitions are allowed and are consequently very fast (a few μs or less). Examples of f–f and d–f emission spectra are given in Fig. 1 and Fig. 2 respectively.

It is interesting to compare the emission properties of rare earth phosphors with other luminescent centres. Many transition metal ions are known as luminescent centres, e.g. Mn^{2+} in Zn_2SiO_4:Mn (Fig. 3). The $^4T_1$ $(t_{2g}^4e_g^1)\rightarrow{}^6A_1(t_{2g}^3e_g^2)$ transition, leading to a green emission in this compound, involves a change in the chemical bonding due to the transition of an electron from the t_{2g} orbitals to the e_g orbitals. Therefore, the emission band is broad. The emission spectrum of Mn^{4+} in

---

*Corresponding author. fax: +49 241 6003442; e-mail: ronda@pfa.research.philips.com

0925-8388/98/$19.00 © 1998 Elsevier Science S.A. All rights reserved.
PII: S0925-8388(98)00416-2

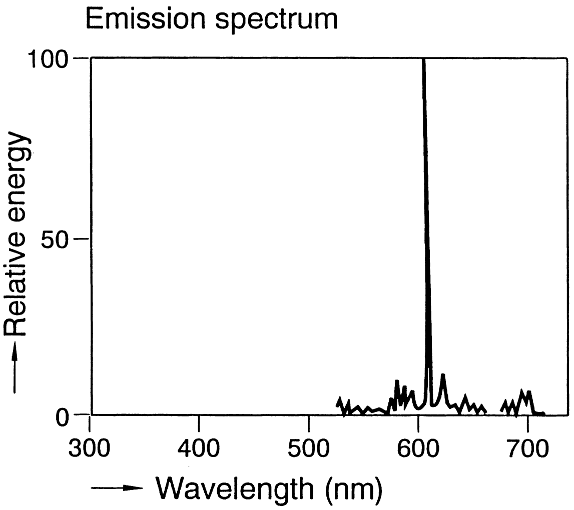

Fig. 1. Emission spectrum of Y_2O_3:Eu.

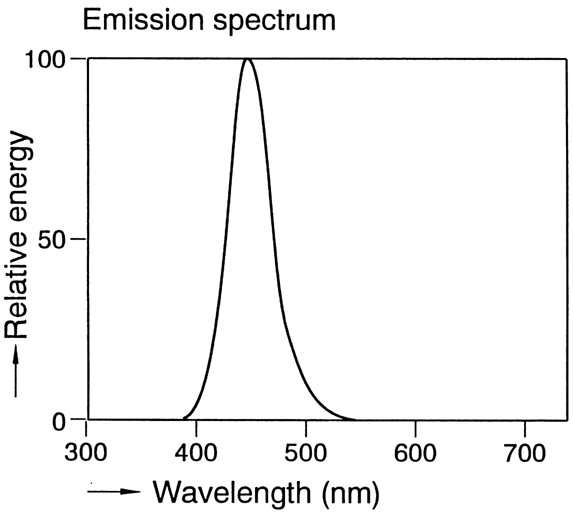

Fig. 2. Emission spectrum of $BaMgAl_{10}O_{17}$:Eu.

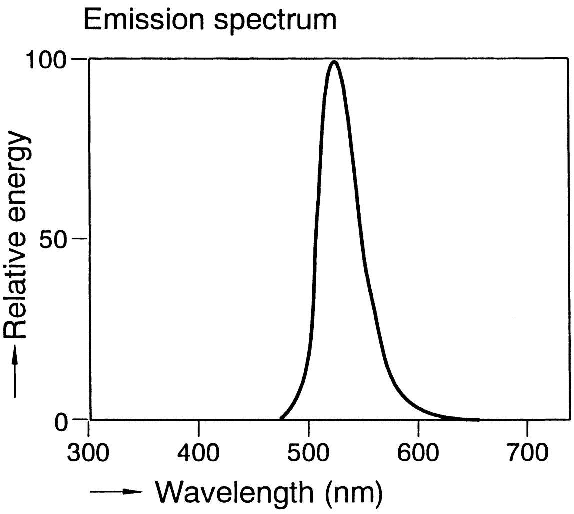

Fig. 3. Emission spectrum of Zn_2SiO_4:Mn.

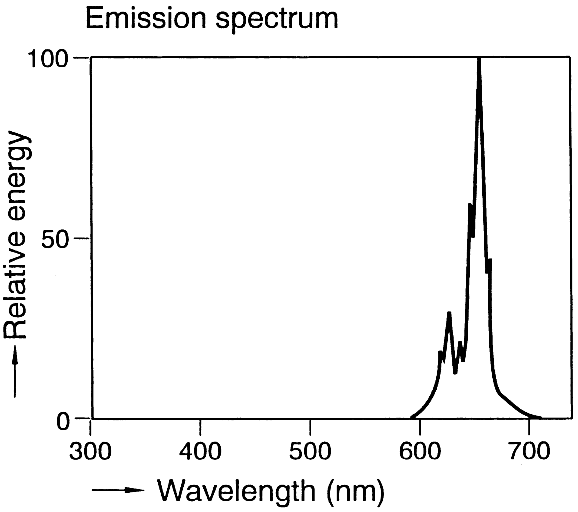

Fig. 4. Emission spectrum of $Mg_4GeO_{5.5}F$:Mn.

$Mg_4GeO_{5.5}F$:Mn (Fig. 4) consists of a relatively narrow emission line with some structure due to vibronic interactions. Here, the emission is due to a spin flip transition within the t_{2g}^3 manifold, i.e. the chemical bonding is hardly changed. This latter example shows that also in cases of optical transitions involving states which participate in the chemical bonding sharp emission bands can be observed when the chemical bond strength in ground- and excited state does not differ significantly.

Emission, originating from complex anions (like in $CaWO_4$, Fig. 5), usually results from a charge transfer transition: a transition involving electronic states of different ions. Here, the chemical bonding will vary strongly, leading to broad emission bands.

The treatment given above shows that line emission is not a specific property of rare earth ions and in addition to that, in the case of rare earth ions, broad emission spectra can be obtained as well, depending on the optical transi-

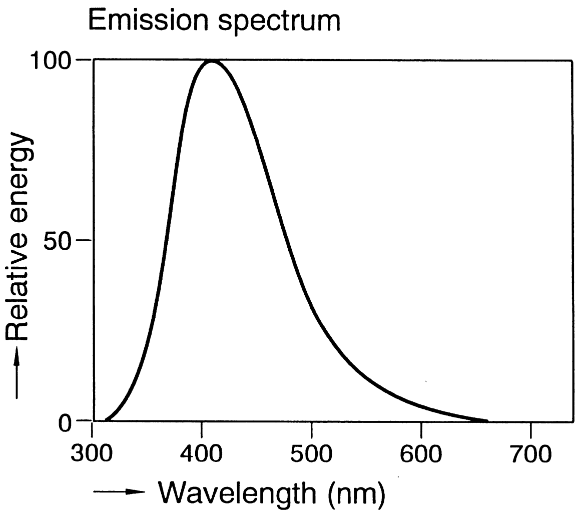

Fig. 5. Emission spectrum of $CaWO_4$.

tions involved. In this respect, rare earth ions are not unique. The unique properties of rare earth ions originate from the fact that the spectral position of the emission lines is almost independent of the host lattice, in contrast to line emission generated by transition metal ions. In addition, some of the line emitting ions (Tb^{3+} and Eu^{3+}) emit at spectral positions, enabling high lumen efficacies and a very good quality of white light (see below): the emission spectra of these ions are adapted to the human eye in a very good way.

3. Excitation and emission properties of applied rare earth phosphors

In this section, we discuss applicational aspects of phosphors for fluorescent lamps and displays.

3.1. Phosphors for fluorescent lamps

We will consider fluorescent lamps for general illumination purposes only, i.e. fluorescent lamps which emit white light. Apart from the efficiency with which white light is generated another important property of lamps is their ability to reproduce all colours in a natural way and also having the colour temperature of the light generated. These factors are determined to a large extent by the phosphors applied. The colour temperature equals the temperature of a black body radiator whose emission spectrum has the same colour coordinates. The so called colour rendering index (CRI) is determined by comparing the emission spectrum of the lamp with that of a black body radiator having the same colour temperature. A black body radiator (and also an incandescent lamp) has a CRI of 100 by definition.

Until about 20 years ago, mainly $Ca_5(PO_4)_3(F,Cl)$:(Sb,Mn) (halophosphate, CHP) was used in fluorescent lamps for general lighting purposes. In this compound, the UV radiation, generated by the Hg discharge, is absorbed by Sb^{3+} and partly transferred to Mn^{2+}. The combination of a blue (Sb^{3+}) and yellow (Mn^{2+}) emission band results in white light. Lamps based on CHP have a moderate energy efficacy (75 lm/W) and a relatively low CRI (50–60).

Rare earth phosphors have changed the situation dramatically. Both the CRI and the energy efficacy of fluorescent lamps based on rare earth emitters are considerably higher than in the case of lamps based on CHP, see e.g. [1]. In such lamps, CRIs larger than 80 can be obtained at efficacies of 100 lm/W, see [2]. Examples for phosphors used in these high quality fluorescent lamps are given below.

$BaMgAl_{10}O_{17}$ doped with Eu^{2+} (BAM) is used as blue emitting phosphor in high quality fluorescent lamps. In this material the photons are absorbed by Eu^{2+} ions, the absorption being due to a 4f→5d transition. The emission takes place on Eu^{2+} as well, the emission originates from the 5d→4f optical transition.

The red emission in these lamps is generated by Y_2O_3:Eu. Here, excitation involves a charge transfer transition from O^{2-} ions to Eu^{3+}. Emission takes place within the f-levels of the Eu^{3+} ions.

It is possible that the optical absorption on a centre showing the desired emission is not strong enough. In such cases, absorption and emission take place on different optical centres. After optical absorption, the energy is transported through the lattice towards the emitting optical centre. All green emitting Tb^{3+} phosphors, applied in high quality fluorescent lamps, rely on optical absorption on Ce^{3+} ions, followed by energy transfer to the emitting Tb^{3+} ions. An example is $(Ce,Tb)MgAl_{11}O_{19}$, where the energy is transferred from Ce^{3+} to Tb^{3+}. Its emission spectrum is given in Fig. 6. Apart from the line emission originating from Tb^{3+}, one also observes a trace of UV emission originating from Ce^{3+}, indicating that the energy transfer probability is slightly below unity. A smaller amount of UV radiation is generated by e.g. $(Ce,Gd,Tb)MgB_5O_{10}$, where energy transfer from Ce^{3+} to Tb^{3+} proceeds via the Gd^{3+} ion sublattice.

3.2. Phosphors for CRTs

In standard CRTs, the only rare earth phosphor applied is the red-emitting Y_2O_2S:Eu. For blue and green, ZnS doped with Ag and Cu, Au, respectively, are applied. The line emission of the Eu^{3+} ions enables a high luminous efficiency of this material despite the relatively low energy efficiency. Especially for red emitting phosphors being line emitters, this is important in view of the rapid decrease in eye sensitivity for light with wavelength larger than 600 nm.

In CRTs applied in projection television, Y_2O_3:Eu is

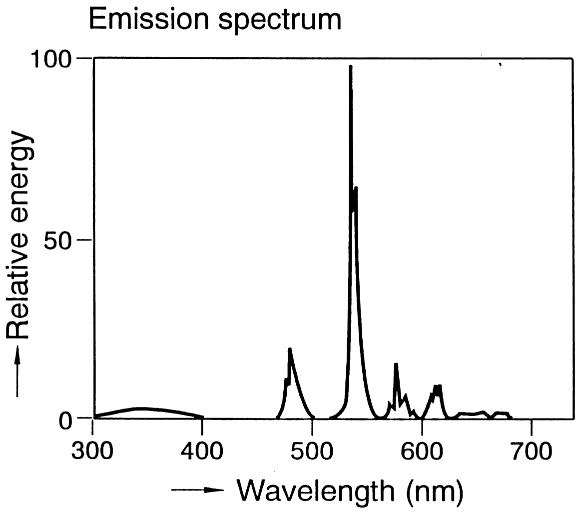

Fig. 6. Emission spectrum of $(Ce,Tb)MgAl_{11}O_{19}$.

applied as red emitting phosphor because it shows a better saturation behaviour than Y_2O_2S:Eu. Here, the green emitting phosphor applied also is a rare earth phosphor; in most cases Y_2SiO_5:Tb is used. Contrary to the ZnS phosphors, the rare earth activator ion concentrations can be chosen relatively high (in the order of 5%, whereas the activator concentrations in ZnS phosphors are in the order of 100–1000 ppm). For blue, no alternatives to ZnS:Ag have been found.

3.3. Phosphors for vacuum ultraviolet excitation

In Plasma Display Panels (PDPs) and a possible new generation of Hg-free fluorescent lamps, a Xe discharge is used to generate UV photons. In this case, the photon energies are in the Vacuum Ultraviolet (VUV) part of the spectrum. Therefore, excitation of the emission generally takes place via the phosphor host lattice, followed by transfer of the energy to activator or sensitiser ions.

It is of interest to compare this excitation mechanism with the excitation mechanism underlying cathode-ray excitation. In the case of cathode-ray (CR) excitation, the final step in the mechanism leading to emission is the generation of bandgap excitations [3], as in the case of PDP phosphors. Therefore one would expect, based on energy transfer arguments, that efficient CR phosphors would also be suitable for application in PDPs. An important difference between CR phosphors, as applied in standard CRTs, and phosphors applied in VUV devices is the penetration depth. In case of CRT phosphors, the penetration depth is about 3 μm for 30 keV excitation, i.e. surface effects, leading to undesired losses, are small. In case of PDP phosphors, where the optical excitation proceeds via host lattice states (bandgap excitation), the penetration depth is less than 1 μm, and consequently considerable surface effects, generally diminishing the efficiency of the material, (see e.g. [4]), can be expected. Such low penetration depths are also encountered in case of phosphors for low voltage excitation. Therefore, taking only energy arguments into account, one would expect phosphors that are efficient in low voltage applications to perform well in PDP applications as well. On the other hand, degradation and saturation effects will be different for different excitation schemes. Further mechanistic studies are worthwhile.

The performance of a number of phosphors under VUV excitation has been reported as early as 1979 [5]. For display applications, blue emitting barium magnesium aluminates, doped with Eu^{2+}, have a good performance, although some degradation occurs during device operation. The degradation results mainly in a colour point shift of the PDP; the contribution to the luminance of the blue emitting primary is low. The origin of the degradation of BAM is not yet clear, however coatings on $BaMgAl_{10}O_{17}$:Eu have been proven to be a promising way out [6,7].

The green primary for PDPs is based on Mn^{2+}; with the emission spectrum of Mn^{2+} in e.g. Zn_2SiO_4:Mn or $(BaO)_x.6Al_2O_3$:Mn being located at the top of the colour triangle a very large colour gamut can be reproduced. A disadvantage of these materials is the fact that the emission is spin forbidden, resulting in too long a decay time for display applications. The spin selection rule can be lifted by magnetic interaction between magnetic ions [8]. In this way, the radiative life time is shortened, enabling faster decay not originating from loss processes. For lamps, Tb^{3+} emission is preferred in view of the high colour quality required.

Red light is generated either by Y_2O_3:Eu or by $(Y,Gd)BO_3$:Eu. The VUV absorption of Y_2O_3:Eu is weaker than that of $(Y,Gd)BO_3:Eu^{3+}$, however, the emission spectrum of Y_2O_3:Eu better matches the EBU requirements for display applications. The emission spectrum of Y_2O_3:Eu has its maximum at 611 nm, whereas the emission spectrum of the mixed borate has its maximum at 595 nm. This nicely illustrates that, though the emission on Eu^{3+} is due to optical transitions within the f-manifold, nevertheless the detailed shape of the emission spectrum depends on the crystal host. In this particular case, the emission at 611 nm in Y_2O_3:Eu originates from an electric dipole transition, whereas the emission at 595 nm in $(Y,Gd)BO_3$:Eu is due to a magnetic dipole transition. In $(Y,Gd)BO_3$:Eu, the electric dipole transitions are symmetry forbidden, as the Eu^{3+} ions are incorporated at a site with inversion symmetry, a fact which is well known. A second consequence is, that the Eu^{3+} emission in $(Y,Gd)BO_3$:Eu is rather slow (3 ms), a disadvantage if being applied in displays.

4. New developments

4.1. Excitation and emission in ternary borates

Recently, we have investigated the absorption- and emission properties of Eu^{3+} doped ternary borates. In the experiments, the overall symmetry of the compounds was not changed (i.e. the structure type was in all cases calcite having trivalent sites with D_{3d} inversion symmetry). The local symmetry, however, was varied by the incorporation of two different kinds of metal ions. We have observed that, though the local symmetry around the Eu^{3+} ions must have been changed, nevertheless the f–f emission spectra do not change significantly, see Fig. 7. Of interest, however, is the fact that the optical absorption at 254 nm strongly depends on the composition of the material, as shown in Fig. 8. The maximum of the optical absorption is located at wavelengths well below 254 nm. In $(Lu_xIn_{1-x})BO_3$:Eu, we observe the strongest absorption of light with wavelength 254 nm for $0.3<x<0.5$. The optical absorption is a charge transfer transition which involves oxygen p states. These states are therefore highly sensitive

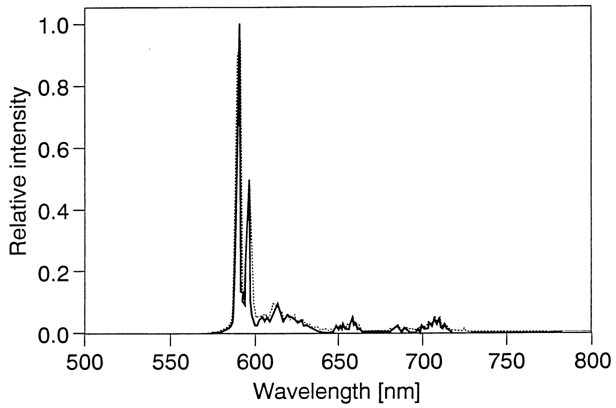

Fig. 7. Comparison of emission spectrum of Eu^{3+} in $LuBO_3$ (continuous line) and $Lu_{0.5}In_{0.5}BO_3$:Eu (dashed line).

to changes of the local environment. We assign the increased absorption to a lifting of the degeneracy of the oxygen p states, originating from a lowering of symmetry in the ternary borates. As a consequence, the p manifold is broadened which results in enhanced absorption of light of 254 nm in a way elucidated in Fig. 9.

4.2. Application of rare earth phosphors in semiconductor LEDs

The invention of the blue light emitting diode (LED) based on GaN can be regarded as a triumph of material chemistry. Electroluminescence based on III–V nitride semiconductors had already been abandoned when S. Nakamura from NICHIA Chemicals picked up the topic again in the late 1980s and developed it within only 5 years to an impressive maturity level. Excellent reviews about the underlying semiconductor photophysics as well as the MOCVD technique used for LED chip production can be found elsewhere [9–11]. The blue diode is capable of challenging the lighting market. For the first time it is possible to generate white light from LEDs with efficiencies equal to halogen lamps.

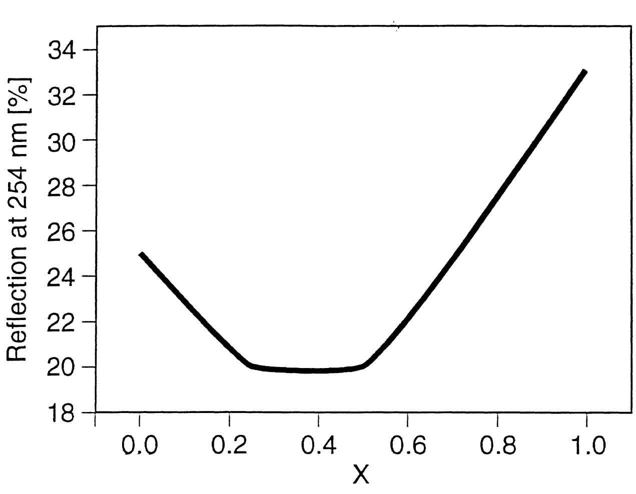

Fig. 8. Reflection of $Lu_xIn_{1-x}BO_3$:Eu at 254 nm as a function of x.

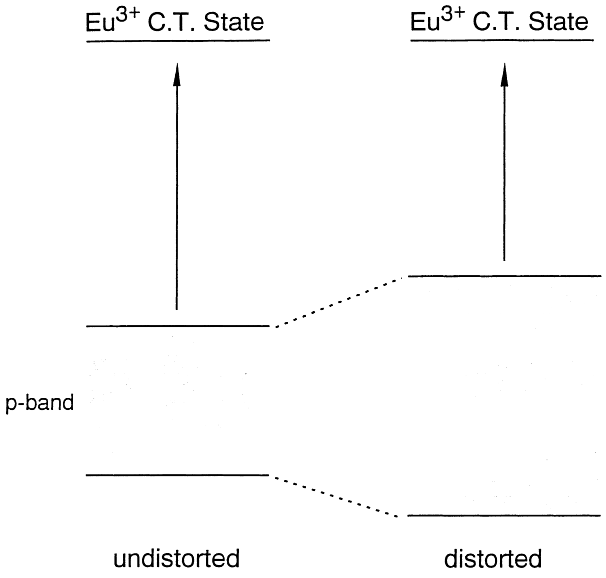

Fig. 9. Broadening of oxygen p-band due to low symmetry distortion, causing increased absorption at 254 nm.

Two ways of white light generation appear likely. First, blue, green, and red diodes can be combined to yield white light. This is attractive since by extending the GaN technique bright green diodes based on AlInGaN are available as well with high external quantum yields. So-called cluster lamps consisting of blue, green, and red LEDs are already on the market. Second, in a very cheap way a single white LED can be obtained by combining a blue LED with green, yellow, and/or red emitting phosphor materials which absorb and convert part of the incident blue light. In comparison to the three LED device this causes a decrease in the overall efficiency because the quantum deficit of the light conversion from blue to yellow/red has to be taken into account. In the following, this option will be discussed with regard to light quality and luminous efficiency.

In principle, it is possible to vary the emission wavelength of blue GaN based LEDs between 370 nm, which marks the bandgap of pure GaN, and 470 nm by increasing the In content in the InGaN devices. Assuming a conversion from the incident light by a phosphor material emitting at 555 nm, the already mentioned quantum deficit decreases in the same direction from about 33% to 15%. At a first glance, the obvious option would therefore be a combination of a blue LED emitting at 470 nm and a broad-band phosphor which can be excited at that wavelength and re-emitting at about 555 nm, creating white light composed of the blue and yellow–green emissions. Such a device has been realized using $(Y_{1-x}Gd_x)_3(Al_{1-y}Ga_y)_5O_{12}$:$Ce^{3+}$ (YAG:Ce) as a broad band yellow phosphor, see Fig. 10. The variation of x and y causes a YAG:Ce emission shift between 510 and 570

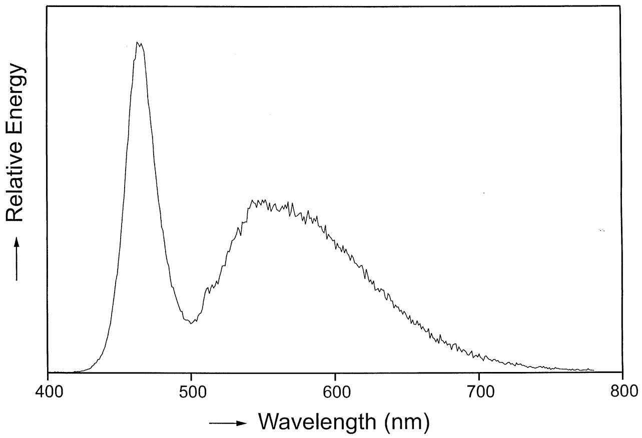

Fig. 10. Emission spectrum of a white LED consisting of a blue LED and yellow emitting YAG:Ce.

nm. This allows the adjustment of white colour temperatures from 8000 down to 3000 K. The former, very high colour temperature has been chosen for commercialization in the Japanese market which demands this colour quality. Due to the broad YAG:Ce emission the CRI is high, reaching CRI=85. Finally, the luminous efficiency is 5 lm/W^9. This is already half of that of an incandescent lamp and shows clearly the potential of the blue LED and its possible importance for the future lighting market. All low-power white light sources which demand long lifetime could possibly be replaced by white LEDs in the medium term. However, it should be pointed out that there are still about 80 such LEDs necessary to replace a 10 W light bulb, assuming a medium power driving scheme of 50 mA at 5 V. The major drawback of this combination is the strongly decreasing overall efficiency upon lowering the colour temperature. This is caused by the broad YAG:Ce emission which, when shifted towards longer wavelength, shows less and less integral overlap with the eye sensitivity curve, hence decreasing in luminous efficacy. This calls for other options which means other phosphor materials or combinations of them. The basic requirements, however, are rather stringent. The phosphor material has to have a sufficient absorption at the emission wavelength of the blue diode, the quantum yield should be high under UV/VIS excitation and the full width at half maximum (FWHM) of the emission band should be as small as possible in order to achieve high luminous output. Selected rare earth phosphors based on Eu^{3+} and Tb^{3+} fulfil the latter two options; however, it can be shown that there is a theoretical low energy limit for the excitation peak maximum wavelength. Even if tight sensitization schemes can be found, i.e. sensitizers with energy levels close to the ^5D terms of Eu^{3+} and Tb^{3+}, these ions cannot be excited with peak wavelength longer than approximately 420 and 370 nm, respectively. This is due to the downward energy cascade which is necessary to effectively sensitise the rare earth ion without back energy transfer [12], taking also the Stokes Shift on the sensitiser into account. Inorganic Eu^{3+} phosphors with high quantum efficiencies which absorb satisfactorily at 370 nm are $Y_2O_2S:Eu^{3+}$ and $Y(V,P,B)O_4:Eu^{3+}$. Tb^{3+} doped material can hardly be found, $(Ce,Tb,Gd)MgB_5O_{10}$ (CBT), mainly used in tubular fluorescent lamps, absorbs only to about 10% at 370 nm. Organic phosphors employing Eu^{3+} and Tb^{3+} coordinated to light-absorbing organic ligands such as acetylacetonate and phenanthroline can be designed to absorb efficiently at 370–400 nm. However, stability and saturation issues have yet to be improved for these materials.

Despite these difficulties and the higher quantum deficit a LED emitting UV light at 370 nm covered with a rare earth phosphor mixture would be an attractive option. In contrast to a phosphor deposited on a blue emitting LED chip at 470 nm which only partly absorbs the blue light in order to generate white light, a mixture of blue, green and red phosphors on a UV LED absorbs all of the incident light emitted by the chip. The white light colour coordinates are determined only by the phosphor portions in the mixture which can be adjusted rather accurately. Consequently, white LEDs can be produced with colour coordinates varying only very little from LED to LED. This is considerably more difficult for an LED from which white light is composed from incident blue emission from the diode and yellow/red light emitted by the phosphor. Deposition of a well-defined phosphor layer on the LED chip of some 1 mm^2 in order to achieve controlled absorption means a real manufacturing challenge (Fig. 11). Further, the additional quantum deficit of about 15% of a colour conversion from 370 nm vs. 470 nm can be compensated considerably by the very high lumen equivalents of Eu^{3+}– and Tb^{3+}-activated phosphors. In analogy

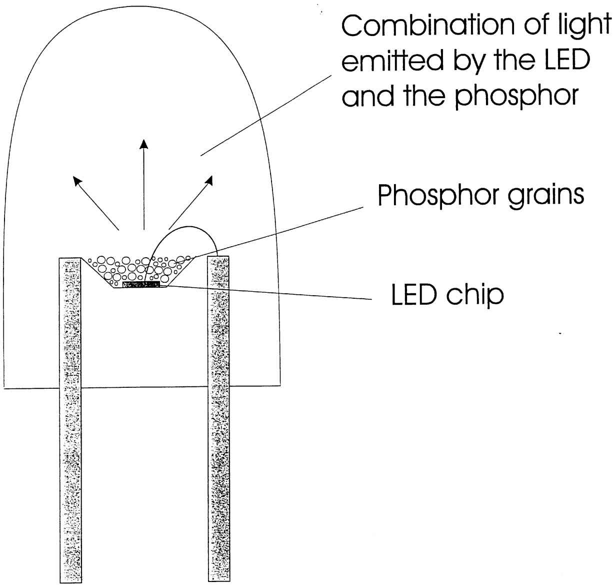

Fig. 11. Sketch of a phosphor-LED lamp.

to fluorescent lamps (see above), high colour renderings can be obtained at the same time. The search for stable inorganic rare earth phosphors with high absorptions in the near UV/blue spectral region is therefore an attractive research task.

4.3. Luminescent materials with quantum yield larger than unity

In 1974, two papers appeared in the same edition of the Journal of Luminescence, on the generation of more than one visible photon out of one UV photon [13,14]. The rare earth ion performing the quantum cutting or quantum splitting was Pr^{3+} in YF_3 as host lattice. It is quite surprising that with UV photons with wavelength of about 200 nm, blue and red emission, originating from Pr^{3+}, can be generated with a quantum efficiency of about 140%. The optical absorption is due to a 4f→5d transition on Pr^{3+} (in this lattice located at about 185 nm). Though a breakthrough, this material has never been applied in fluorescent lamps. An important reason is the fact that the blue line emission, generated by Pr^{3+}, is located at about 410 nm and therefore not suitable for lamps with good colour rendering. The red emission, also generated by the Pr^{3+} in the cascade leading to quantum cutting has very good spectral properties for high quality fluorescent lamps; it is located at about 620 nm.

Quite recently, Srivastava et al. reported the observation of the blue line emission of Pr^{3+} in oxidic materials in which the rare earth ion is coordinated by a large number of oxygen ions (like in $SrAl_{12}O_{19}$, where the Pr^{3+} is coordinated by 12 oxygen ions) [15,16]. A prerequisite for the observation of blue emission is that the energy of the 5d level is higher than that of the highest 4f level, from which the blue emission originates. By choosing a high rare earth ion coordination number, the mean metal–ligand distance becomes large. The crystal field splitting decreases on increasing the metal–ligand distance. As a consequence, in $SrAl_{12}O_{19}$ the Pr^{3+} ion experiences such a weak crystal field that indeed the energy position of the lowest 5d level is higher than that of the highest 4f level, a situation until then only observed in fluorides. Again, this can be regarded as a breakthrough, however the question concerning the blue line emission at 410 nm is not solved. A possible solution is the use of additional phosphors showing a strong absorption in the blue-UV part of the optical spectrum and which emit light with longer wavelength, in the same manner as discussed above. In this way, also the very deep blue Pr^{3+} emission could be utilized.

In 1997, Meijerink et al. published a luminescent material ($LiGdF_4$:Eu) with a quantum efficiency of almost 200%; the emission originating almost exclusively from Eu^{3+} [17]. Excitation with VUV radiation is on the Gd^{3+} ion, using radiation with a wavelength of about 160 nm. In the first step, Eu^{3+} ions are excited via cross relaxation between Gd^{3+} and Eu^{3+}. (We remark that the authors also observed orange–red emission, originating from Gd^{3+} in this compound when not doped with Eu^{3+} [18]). In the second step, Eu^{3+} ions are excited via energy transfer from Gd^{3+}→Eu^{3+}, see Fig. 12. This is the first material showing such a high quantum efficiency on excitation with radiation with wavelength longer than 100 nm.

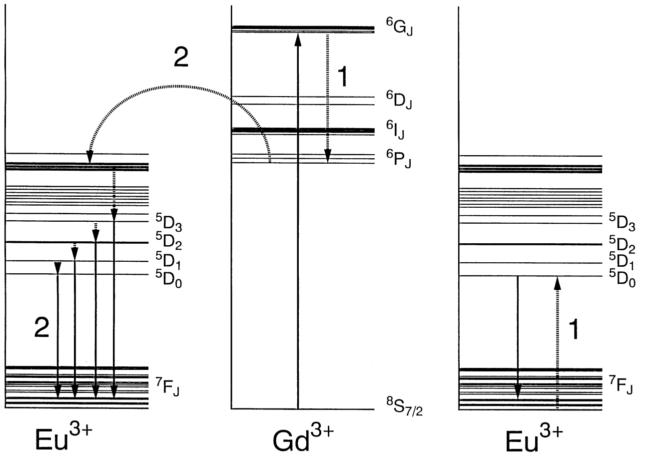

Fig. 12. Processes leading to quantum cutting in $LiGdF_4$:Eu.

5. Conclusions

In many applications, the performance of rare earth phosphors is almost ideal and consequently the use of rare earth phosphors has pushed the performance of devices based on them to their physical limits. New impetus for research on phosphors is expected from new applications like luminescent materials applied in LEDs or phosphors showing new features e.g. exhibiting quantum efficiencies larger than unity.

References

[1] M. Koedam, J.J. Opstelten, Light Res. Techn. 3 (1971) 295.
[2] C.R. Ronda, J. Lumin. 72-74 (1997) 49.
[3] D.J. Robbins, J. Electrochem. Soc. 127 (1980) 2694.
[4] D.B.M. Klaassen, H. Mulder, C.R. Ronda, Phys. Rev. B 39 (1989) 42.
[5] NHK Technical Monograph 28 (1979).
[6] H. Bechtel, W. Czarnojan, W. Mayr, T. Jüstel, H. Nikol, C. Ronda, German Patent 19727607.5, 1997.
[7] C.R. Ronda, Proc. 2nd Int. Display Workshops, Vol. 1, Hamamatsu, Japan, 1995, p. 69.
[8] C.R. Ronda, T. Amrein, J. Lumin. 69 (1996) 245.
[9] S. Nakamura, G. Fasol, The Blue Laser Diode, Springer, Berlin, 1997.
[10] T. Matsuoka, Adv. Mater. 8 (1996) 469.
[11] S. Strite, The III–V nitride semiconductors for blue light emission, in: H.-J. Queisser (Ed.), Advances in Solid State Festkörperprobleme Series, Springer, 1994.

[12] V. Balzani, F. Scandola, Supramolecular Chemistry Ellis Horwood, New York, 1991.

[13] W.W. Piper, J.A. DeLuca, F.S. Ham, J. Lumin. 8 (1974) 344.

[14] J. L Sommerdijk, A. Bril, A.W. de Jager, J. Lumin. 8 (1974) 341.

[15] A.M. Srivastava, W.W. Beers, J. Lumin. 71 (1997) 285.

[16] A.M. Srivastava, D.A. Doughty, W.W. Beers, J. Electrochem. Soc. 143 (1996) 4113.

[17] R.T. Wegh, H. Donker, A. Meijerink, Book of Extended Abstracts of the 192nd Meeting of the Electrochemical Society, Paris France, 1997, p. 1766.

[18] R.T. Wegh, H. Donker, A. Meijerink, R.J. Lamminmäki, Hölsa, J., submitted to Phys, Rev. B 56 (1997) 13841.